Classical and quantal pseudoergodic regions of the Henon–Heiles system

Kenneth G. Kay
Department of Chemistry, Kansas State University, Manhattan, Kansas 66506 and Department of Chemistry, Bar-Ilan University, Ramat-Gan, Israel 52100[a]

B. Ramachandran
Department of Chemistry, Kansas State University, Manhattan, Kansas 66506[b]

(Received 17 November 1987; accepted 7 January 1988)

This work describes an approximate and temporary form of ergodicity, called pseudoergodicity. This is a classical phenomenon that is of particular interest since it has a straightforward quantum analog and can be expected to influence the dynamics of a quantum system more directly than rigorous ergodicity. A procedure is described for locating phase space regions where classical motion is pseudoergodic (pe) and this technique is applied to the Henon–Heiles system excited to near its escape energy. Certain pe zones containing chaotic trajectories appear to coincide with the vague tori of Reinhardt and co-workers while other such zones have less familiar forms. When the Henon–Heiles system is observed for long times, a single pe region becomes larger than others, thus marking incipient ergodicity on much of the energy shell. The classical pe regions are compared to quantum pe zones, calculated by a slight modification of a technique presented in an earlier paper. It is found that certain classical pe regions have close quantum analogs while others do not, for reasons probably related to the short time scale for quantum-classical correspondence. Among the classical regions that do not have quantum analogs is the aforementioned dominant pe zone. The implication is that the present quantum system does not display behavior similar to the truly large-scale ergodicity that occurs in the classical system.

I. INTRODUCTION

Ergodicity[1–3] is a fundamental concept in classical mechanics. Motion of a classical system is always ergodic in some portion of phase space[4] and the region of ergodicity serves to characterize the motion. Ergodicity over the region constituting the entire energy surface is one of the conditions which lead to the validity of various statistical theories.[5] The importance of the notion of ergodicity is, thus, self-evident.

Ergodicity, however, is basically a classical concept. There does not exist a unique, truly analogous counterpart to this notion in quantum mechanics. Although it is possible to identify the consequences of ergodicity for a quantum system in the classical limit,[6–8] it is not possible to extend this analysis rigorously to systems with $\hbar > 0$. Thus, a definition of ergodicity can be presented for quantum systems[2,9–11] only by abandoning the vital requirement that it tend to the classical definition as $\hbar \to 0$ or by introducing arbitrary elements or auxilliary hypotheses that are not strictly related to ergodicity.

Despite the specifically classical nature of ergodicity, however, the Bohr correspondence principle suggests that the evolution of a quantum system with small enough $\hbar$ should resemble that of its classical counterpart. In particular, a quantum system that is close enough to the classical limit should display behavior that is, *in some sense*, similar to the ergodic behavior of its classical analog. It is clearly of interest to specify more precisely the sense in which quantum evolution can mimic ergodic behavior and to measure the extent to which this actually occurs in given cases. To enable such judgments, we have found it useful, in earlier work,[12] to introduce an approximate form of ergodicity called *psuedoergodicity* (pe). Pseudoergodicity is an especially helpful concept because it can be made to approach strict ergodicity as closely as desired but has a quantum analog that is much freer from ambiguity than that of ergodicity. Thus, it is much more straightforward to compare pe behavior in quantum and classical systems than it is to make similar comparisons about ergodicity. With the introduction of pe, one judges how well ergodicity is reflected in the dynamics of a quantum system by a two-step process: one compares quantum pe to classical pe and then compares classical pe to ergodicity.

In our earlier work,[12] we performed rather extensive calculations of pe for a particular quantum system—the quantum Henon–Heiles[13] system. However, those calculations were not accompanied by comparative classical studies. In this paper, we describe a practical technique for performing classical computations of pe and apply this method to the classical version of the Henon–Heiles system.[14] These calculations establish the classical interpretation of the quantum results, provide a clearer idea of the extent of ergodic behavior in a quantum system, and reveal some interesting classical phenomena.

The plan for the remainder of this paper is as follows. In Sec. II we review the classical concept of ergodicity. In Sec. III we use these ideas to develop the notion of pseudoergodicity. In Sec. IV we present a practical technique for performing classical calculations of pe and apply this procedure to the Henon–Heiles system. In Secs. V and VI we, respectively, present the results of these calculations and compare

[a] Address for correspondence and reprints.
[b] Current address: Department of Chemistry and Institute for Theoretical Chemistry, University of Texas, Austin, Texas 78712.

 0021-9606/88/095688-16$02.10

them to those of analogous quantum calculations. Finally, in Sec. VII, we summarize our work and offer our conclusions.

II. CLASSICAL ERGODICITY

The review of classical ergodicity presented here will help us relate the definition of pe to that of ergodicity and will lead to a procedure for performing calculations of pe.

We consider an autonomous, bound, physical system described by the Hamiltonian $H(\mathbf{p},\mathbf{q})$, where $\mathbf{p}$ and $\mathbf{q}$ are, respectively, momenta and coordinates. To define ergodicity, we must introduce the idea of an invariant region $\mathscr{R}$ in phase space. This is a portion of the energy surface that is carried into itself by the dynamical evolution of the physical system. Trajectories never cross the boundaries of $\mathscr{R}$, so that points initially within $\mathscr{R}$ never leave this region while points outside of $\mathscr{R}$ never enter it. We associate a density function ρ,

$$\rho(\mathbf{p},\mathbf{q}) = \delta[E - H(\mathbf{p},\mathbf{q})]\chi(\mathbf{p},\mathbf{q}) \tag{1}$$

with the invariant region, where the delta function places the density on the energy surface $H(\mathbf{p},\mathbf{q}) = E$, while the characteristic function

$$\chi(\mathbf{p},\mathbf{q}) = \begin{cases} 1 & \text{for } (\mathbf{p},\mathbf{q}) \in \mathscr{R} \\ 0 & \text{otherwise} \end{cases} \tag{2}$$

picks out points on the energy surface that are within $\mathscr{R}$. Note that the specification of $\mathscr{R}$ as an invariant region implies that ρ is independent of time:

$$\rho(\mathbf{p}(t),\mathbf{q}(t)) = \rho(\mathbf{p},\mathbf{q}) . \tag{3}$$

We identify the phase space average of a dynamical function $A(\mathbf{p},\mathbf{q})$ over $\mathscr{R}$ as

$$\langle A \rangle = \int d\mathbf{p} \int d\mathbf{q}\, \rho(\mathbf{p},\mathbf{q}) A(\mathbf{p},\mathbf{q}) \Big/ \int d\mathbf{p} \int d\mathbf{q}\, \rho(\mathbf{p},\mathbf{q}) . \tag{4}$$

Although such phase integrals should be properly expressed in terms of Lebesgue integrals, we adopt the above lax notation to make the comparison with the quantum definitions more transparent.

We are now in a position to define ergodicity. Let $A(t)$ denote $A(\mathbf{p}(t),\mathbf{q}(t))$, the function A that is obtained by allowing the coordinates and momenta of the system to evolve from initial values $(\mathbf{p},\mathbf{q})$ at time 0 to the values $(\mathbf{p}(t),\mathbf{q}(t))$ at time t. Futhermore, let

$$\overline{f(t)}^{\,T} = (1/T) \int_0^\infty \exp(-t/T) f(t) dt \tag{5}$$

represent the (exponentially weighted) time average of function $f(t)$. Then the evolution of the system is said to be ergodic in region $\mathscr{R}$ if

$$\lim_{T\to\infty} \overline{\langle A(t)^* A \rangle}^{\,T} = |\langle A \rangle|^2 \tag{6}$$

for all $A \in L^2$, i.e., for all functions obeying

$$\langle |A|^2 \rangle < \infty . \tag{7}$$

This definition relates ergodic behavior to the decay of the time-averaged autocorrelation functions $\overline{\langle A(t)^* A \rangle}^{\,T}$ to their statistical equilibrium values $|\langle A \rangle|^2$. Although Eq. (6) seems to differ from a more conventional definition of ergodicity that is expressed in terms of the unweighted time average,[3] we have shown elsewhere[8] that these definitions are, in fact, equivalent.

Equation (6) can be cast into the interesting form

$$\lim_{T\to\infty} \langle\, |\overline{A(t)}^{\,T} - \langle A \rangle|^2 \rangle = 0 \tag{8}$$

by performing a few elementary steps and applying the invariance of $\mathscr{R}$. We may deduce from this result that ergodicity implies that time averages of all L^2 properties converge to their phase space averages in the L^2 mean. It is possible to derive a stronger result by applying further analysis.[3] It can be shown that ergodicity implies that

$$\lim_{T\to\infty} \overline{A(t)}^{\,T} = \langle A \rangle \tag{9}$$

for almost all points $(\mathbf{p},\mathbf{q})$ in $\mathscr{R}$ and all functions $A \in L^2$. This equation is often quoted as the primary definition of ergodicity.

From a physical standpoint, Eqs. (8) and (9) reveal the same crucial feature of ergodicity: the independence of infinite-time averages from initial conditions chosen in the region. Performing the infinite time average of $A(\mathbf{p},\mathbf{q})$ along almost any trajectory in $\mathscr{R}$ yields the same value $\overline{A(t)}^{\,T}$. This value is just the phase-space average $\langle A \rangle$ or, equivalently (due to invariance of $\mathscr{R}$), $\langle \overline{A(t)}^{\,T} \rangle$.

More valuable insight into ergodicity is provided by Birkhoff's theorem[1-3] which states that ergodicity is equivalent to the metrical indecomposability of $\mathscr{R}$. This means that motion in $\mathscr{R}$ is ergodic if and only if this region cannot be broken down into two invariant regions, each of nonzero measure. The immediate implication is that ergodicity is, indeed, ubiquitous: all motion is ergodic in *some* portion of phase space.[4] In rough terms, the region explored by each trajectory defines a zone of ergodicity. Under these circumstances, the only issue that remains to be settled is the identity of the various ergodic regions of a system.

Actually, the definitions of Eqs. (8) and (9) provide a way to find the ergodic zones, in principle. Since ergodicity is associated with independence of time averages from initial conditions, we could imagine initiating trajectories from each point $(\mathbf{p},\mathbf{q})$ on the energy surface and computing the infinite time averages $\overline{A(\mathbf{p}(t),\mathbf{q}(t))}^{\,\infty}$. Points $(\mathbf{p},\mathbf{q})$ for which $\overline{A(\mathbf{p}(t),\mathbf{q}(t))}^{\,\infty}$ are identical, for all $A \in L^2$, belong to the same ergodic region. Although this is obviously not a practical procedure, it illustrates ideas that we will exploit later when we discuss pe.

It is important to discuss briefly the relationship between ergodicity and the conventional statistical theories of unimolecular chemical kinetics.[5] These theories are based on the fundamental assumption that a form of statistical equilibration, involving all the quasibound states on the energy shell of an isolated molecule, occurs prior to reaction. If this equilibration process results in the statistical relaxation of all L^2 functions $A(\mathbf{p},\mathbf{q})$, then, in the limit of low reaction rates, these theories imply a "global" form of ergodicity, i.e., ergodicity in a region $\mathscr{R}$ of molecular phase space that corresponds to the entire bound portion of the energy surface. In contrast, the form of ergodic behavior we discuss in this paper is "local"—it applies to a region $\mathscr{R}$ that is a limited por-

tion of the bound energy surface. Although this form of ergodicity is not closely related to the usual statistical theories, it is, by far, the most common form of ergodic behavior and is, therefore, a worthy subject for investigation.

It is also important for our discussion to relate ergodicity to chaos.[4] Since all motion—even the regular motion of a completely integrable system—is ergodic in some region $\mathscr{R}$, it is clear that ergodicity does not imply chaos. However, given an ergodic region, there is a simple diagnostic to determine whether the motion therein is chaotic. In the case of regular motion of a system with more than one degree of freedom, the ergodic regions are invariant tori having lower dimension than the full energy surface. Thus, the Liouville measure of the ergodic regions is zero. In the case of chaotic motion, however, the ergodic regions are not confined to low-dimensional portions of the energy surface, except in special circumstances.[15–18] The Liouville measure of chaotic ergodic regions is thus expected to be positive (although generally less than the measure of the full energy surface). Therefore, it is the measure of the region $\mathscr{R}$ that indicates the chaotic or regular nature of the motion. In the present work, we are especially concerned with ergodic regions associated with chaotic motion since we are interested in the consequences of chaos for quantum mechanics.

III. CLASSICAL PSEUDOERGODICITY

The discussion of the previous section makes it clear why ergodic behavior of a classical system does not imply strictly analogous behavior in its quantum counterpart. Classical ergodicity is a property of the dynamics averaged over an infinite time period. However, for nonlinear systems in general and chaotic systems in particular, the behavior predicted by quantum mechanics differs greatly from that obtained by classical mechanics after a finite time has elapsed.[8,9] Thus, it is futile to expect the ergodicity of a typical classical system to be reflected in the dynamics of its quantum counterpart in a completely faithful manner.

Despite this conclusion, we should expect certain indications of classical ergodic behavior to show up in a quantum system under appropriate circumstances, even if the symptoms are not completely free of ambiguity. After all, even though quantum and classical dynamics differ greatly over long time periods, they often agree very well for short time periods.[19] Thus, if ergodic behavior of a classical system is approximately established on a short enough time scale (e.g., if time averages converge quickly enough to phase space averages) some consequences of this behavior should appear in the quantum system. Such approximate ergodicity, established in a finite time period, is called pseudoergodicity. It is a phenomenon that can be realized in both classical and quantum mechanics.

To define pseudoergodicity more precisely, we introduce the quantity[12,20]

$$F_A(T) = [\,\overline{\langle A(t)^* A\rangle}^{\,T} - |\langle A\rangle|^2]/[\langle |A|^2\rangle - |\langle A\rangle|^2]\,, \tag{10}$$

where, as before, the brackets denote the phase space average over the invariant region $\mathscr{R}$. The interest in F_A arises from the following properties[20]:

(1) $1 \geqslant F_A(T) \geqslant 0$ for all T;
(2) $F_A(0) = 1$;
(3) $F_A(T)$ is a monotonically nonincreasing function of T;
(4) $F_A(T) = 1$ for all T, for some $A \in L^2$ (excluding functions of H) if and only if the motion in $\mathscr{R}$ is nonergodic;
(5) $F_A(\infty) = 0$ for all $A \in L^2$ (apart from functions of H), if and only if the motion in $\mathscr{R}$ is ergodic.

Thus, the ergodic or nonergodic nature of the evolution can be deduced from the values of $F_A(\infty)$, determined for all dynamical functions $A \in L^2$ except for functions of the Hamiltonian. For each such A, $F_A(\infty)$ will have a value between 0 and 1. The evolution of the system is ergodic if and only if this limiting value is 0 for every such A.

It is now easy to make a transition to pe. We say that the motion in an *approximately* invariant region $\mathscr{R}$ is pseudoergodic with respect to time $\tau < \infty$, cutoff $0 \leqslant \phi \leqslant 1$, and set of properties $\mathscr{A} \subset L^2$ if

$$F_A(\tau) < \phi \tag{11}$$

for all $A \in \mathscr{A}$. By approximately invariant, we mean that, although $\rho(\mathbf{p}(t),\mathbf{q}(t))$ may not be truly constant in time, it varies slowly enough over time τ that replacement of $\rho(\mathbf{p},\mathbf{q})$ in the numerator of Eq. (10) by its time average $\overline{\rho(\mathbf{p}(t),\mathbf{q}(t))}^{\,\tau}$ would not affect the validity of Eq. (11).

Let us briefly review and discuss the aspects that distinguish the above definition from that of ergodicity.

(1) The finite value of τ. The time τ for the evaluation of the F_A in Eq. (11) has been made finite so that observation of the dynamics can be confined to the time scale over which classical and quantum dynamics are similar. This condition is necessary for our goal of identifying a form of classical behavior that will be reflected in the evolution of its quantum counterpart. As mentioned earlier, the association of ergodicity with infinite-time behavior prevents ergodicity from being faithfully mirrored in quantum mechanics.

(2) The nonzero cutoff ϕ. It is necessary to replace the condition $F_A = 0$ with the more lenient one of Eq. (11) since F_A will not generally attain the asymptotic value of zero in the finite time τ even when the motion in $\mathscr{R}$ is rigorously ergodic.

(3) The restricted set of functions $\mathscr{A}$. We have confined application of the pe criterion to a subset $\mathscr{A}$ of L^2 functions for two reasons: (a) there exist functions $A \in L^2$ that are so highly convoluted or localized that $F_A(\tau)$ evolves arbitrarily slowly and remains arbitrarily close as to 1 for any fixed τ; (b) functions $A \in L^2$ that are too highly localized in phase space evolve very differently according to quantum and classical mechanics, even over short time periods. Thus, the pe condition will never be obeyed classically and will not be suitable for the desired quantum-classical comparisons unless we restrict the class of allowable phase space functions. We note that the requirement that the functions A be not too highly localized (i.e., that their analogous quantum operators effectively project onto more than one quantum state) implies that it is possible to construct a finite (though possibly very large) "complete" set of "independent" functions that "spans" all conceivable members of $\mathscr{A}$. Adding new

nonlocalized functions to this set will not change the resulting pe regions. The set $\mathscr{A}$, with respect to which pe is defined may, but need not, be this complete set.

(4) The approximate invariance of $\mathscr{R}$. We have replaced strict invariance of $\mathscr{R}$ with approximate invariance to achieve consistency with the above three modifications of the ergodicity condition. Since the time τ for examination of the system is now finite, we can relax the requirement of invariance to apply to this time range. In addition, since the restriction on the set of functions A and the nonzero value of ϕ introduce a further looseness in the definition of pe, we are able to relax the invariance requirement further without causing the pe concept to loose its physical interest.

Specifically, the approximate invariance property allows us to carry out steps that are analogous to those leading from Eq. (6) to Eq. (8) in the case of ergodicity. Proceeding in that manner, we obtain the following interesting new form for F_A:

$$F_A(\tau) = \langle | \overline{A(t)}^{\tau} - \langle \overline{A(t)}^{\tau} \rangle |^2 \rangle / \langle |A - \langle A \rangle|^2 \rangle \ . \quad (12)$$

We can see from this expression that pe condition, $F_A(\tau) < \phi$, implies that the variances in time averaged functions $\overline{A(\mathbf{p}(t),\mathbf{q}(t))}^{\tau}$ are smaller than those of the unaveraged functions $A(\mathbf{p},\mathbf{q})$ by the factor ϕ. Put another way, a pe region is a portion of phase space where time averaging decreases the variances in the functions A by a certain factor. Thus, although pe does not require (as does ergodicity) that the time averages of A be strictly constant almost everywhere in $\mathscr{R}$, it does require that they be nearly constant in $\mathscr{R}$ in the sense that their variances be small.

It is worthwhile to restate the definition of pe in a few additional, physically transparent, ways. In rough terms, a pe zone is an almost-invariant part of phase space that is explored by a set of "similar" trajectories during a finite time τ. Equivalently, a pe region is a nearly invariant portion of phase space that consists of points close to a single trajectory of finite duration. This last restatement brings out the similarity between the definition of pe and that of "quasiergodicity"[2] which requires that an arbitrary trajectory in an invariant region come arbitrarily close to every other point in that region in the course of an infinite time period.

These different ways of understanding pe help emphasize that this phenomenon is expected to occur quite generally in a region that remains nearly invariant long enough for a typical trajectory to sample a large part of it. Such approximate invariance may be caused by the presence of "bottlenecks"[21,22] which temporarily confine the phase space flow to certain parts of the energy surface. We, therefore, anticipate that pe regions will sometimes be associated with bottlenecks and their various manifestations, including "vague tori."[23]

It is possible to make the pe condition approach that of ergodicity as closely as we wish by choosing τ to be sufficiently large, ϕ to be sufficiently small, and by suitably enlarging the set $\mathscr{A}$. However, as long as the appropriate limits have not been achieved, pe and ergodicity are not the same. We now turn our attention to the differences between these two concepts.

First, it is necessary to understand that pseudoergodicity does not imply ergodicity. There are at least two reasons for this:

(a) Although $\mathscr{R}$ may be approximately invariant, it is generally not truly invariant. For example, a region enclosed by bottlenecks is not truly invariant since the bottlenecks restrict the system's motion for only a limited time. If τ is chosen to be sufficiently small, the region may satisfy the approximate invariance condition and the motion therein may qualify as pe. However, since the system's trajectories eventually cross the bottlenecks, this region is not truly invariant and the motion cannot be ergodic in this portion of space.

(b) The dynamics in a region may qualify as pe only because the set $\mathscr{A}$ of functions is limited. It is possible that calculation of $F_A(T)$ for L^2 functions that are omitted from $\mathscr{A}$ would yield nonzero values as $T \to \infty$, thus signifying nonergodic behavior.

It is also important to realize that ergodicity does not generally imply pseudoergodicity for a particular choice of τ, ϕ, and $\mathscr{A}$. The convergence of $F_A(T)$ to zero implied by ergodicity may be too slow for the pe condition [Eq. (11)] to be obeyed.

A final feature of pe that distinguishes it from ergodicity concerns the nature of the phase space regions wherein the motion is pe or ergodic. The equivalence of ergodicity to metrical indecomposability implies that ergodic regions are uniquely defined and that different ergodic regions are disjoint. The absence of a relationship between pe and metrical indecomposability, however, leaves pe zones with vaguely defined boundaries and allows points in phase space simultaneously to belong to more than one such region. Thus, there is no unique partitioning of phase space into pe regions and different pe zones may overlap. Although it is possible to impose additional conditions on pe regions in an attempt to define them more sharply (see below), these do not change their fundamental vagueness. The lack of uniqueness of the partitioning of phase space into pe regions is the most disturbing feature of pe.

As the above discussion makes clear, the concept of pe is not as powerful or robust as that of ergodicity. The price for relaxing the conditions of ergodicity may be high but it must be paid if we wish to identify a form of behavior in a classical system that bears some relation to ergodicity and yet can directly influence the dynamics of its quantum counterpart.

IV. CALCULATIONS

We now illustrate the notion of pe by describing calculations on the well-known Henon–Heiles[13] system, defined by the Hamiltonian

$$H = \tfrac{1}{2}(p_x^2 + x^2 + p_y^2 + y^2) + \lambda(xy^2 - \tfrac{1}{3}x^3) \quad (13)$$

with λ chosen to be 0.08. The escape energy for this system is 26.04.

The set $\mathscr{A}$ for our calculations is chosen to consist of the following five functions:

$$D = \tfrac{1}{2}(p_x^2 + x^2 - p_y^2 - y^2) \ , \quad (14a)$$

$$P = p_x p_y + xy \ , \quad (14b)$$

$$L = xp_y - yp_x \ , \quad (14c)$$

$$L^2 = (xp_y - yp_x)^2, \tag{14d}$$

and

$$H_0 = \tfrac{1}{2}(p_x^2 + x^2 + p_y^2 + y^2). \tag{14e}$$

Since the Poisson bracket of the separable, zero-order, Hamiltonian H_0 with each of these functions vanishes, these functions are zero-order constants of motion. The condition $F_A < \phi$ implies the destruction of these constants, as is consistent with chaotic behavior. Apart from the function P, these same functions were used in our earlier quantum mechanical study of pe. Although the above five quantities by no means constitute the "complete" set of not too strongly localized functions, discussed in the previous section, they are certainly members of that set and form a valid choice for $\mathscr{A}$.

To facilitate comparisons with our previous quantum work,[12] we carry out our classical calculations with the parameter ϕ set to 0.04. Our quantum studies suggested that values of ϕ in this range produce pe regions that coincide with chaotic zones of phase space.[24] From the viewpoint being developed here, however, the value 0.04 is arbitrary and any other value could be used.

Again, to allow straightforward comparisons with the earlier quantum computations,[12] we choose the observation time τ to be 30 time units for most of our classical calculations. We do, however, briefly investigate the effect of varying this parameter in the range of 15 to 130 units.

As discussed in Ref. 12 and reviewed in Sec. VI, the quantum mechanical analog of a pe region is a set of states. Furthermore, this set must consist of at least two members. To maintain a close analogy to these quantum regions, the classical pe zones obtained here are required to occupy a correspondingly large portion of phase space. Thus, pe zones that occupy a volume of phase space that is smaller than about $2h^2$ are neglected in the present classical calculations.

The invariance condition described in the previous section is rather difficult to impose in either the classical calculations or in their quantum mechanical counterparts. Therefore, for our actual calculations, we have replaced this condition with one that is more easily applied. We have required that the density function $\rho(\mathbf{p},\mathbf{q})$ for region $\mathscr{R}$ be nearly independent of time in the sense that

$$|\overline{\langle A(t)\rangle}^{\tau} - \langle A\rangle| / [\langle |A|^2\rangle - |\langle A\rangle|^2]^{1/2} < \beta\phi^{1/2} \tag{15}$$

for all $A \in \mathscr{A}$, where β is a number which we have chosen as 1 for our calculations. The relationship of Eq. (15) to the invariance condition of the previous section is as follows: if Eq. (15) is imposed not only in its present form (with a suitably small value of β) but also with the functions $A(t)$ and A in the numerator replaced by $A(t)^*A$ and $|A|^2$, respectively, then the previously stated invariance condition will also be obeyed. We point out that the replacement of the original invariance condition by Eq. (15) does not affect the validity of our quantum-classical comparisons since our quantum mechanical calculations apply an invariance condition that is analogous to Eq. (15).

The computational procedure for locating the pe zones is a suitably modified version of the idealized method for finding ergodic regions described in the previous section. A more detailed description is presented in the Appendix, but a rough outline is as follows: First, we scatter points at random on the energy surface of the system. Next, we evolve trajectories from each of these points and calculate the time averages along these trajectories of the functions in $\mathscr{A}$. Finally, we group together trajectories with similar values for the time averages, compute phase-space averages of the functions for these groups, and add or remove trajectories from the groups until the conditions for pe [$F_A(\tau) < \phi$, with F_A given by Eq. (12)] and invariance [Eq. (15)] are obeyed.

It is important to mention two details of this procedure which impose requirements on pe zones that extend beyond those we have previously described. First, when we collect trajectories with similar values of the time averages, we attempt to include as many trajectories as possible in these groups, subject to the pe and invariance conditions. This has the effect of making the pe regions as large as possible. Second, we identify the pe regions one at a time and, when we locate such a region, we exclude the corresponding trajectories from consideration for the formation of further pe zones. This produces pe regions that are disjoint. The maximum-size and disjointness properties of the pe regions neither conflict with the definition of pe presented above, nor necessarily follow from it. They are new requirements that remove some of the arbitrariness in the specification of the pe regions inherent in Eq. (11).

These new conditions, however, still do not lead to uniquely defined regions. The remaining nonuniqueness shows up as a dependence of the pe zones upon another detail of the computational procedure. In the calculations, the functions A in $\mathscr{A}$ are considered in a particular order and the groups of trajectories are subjected to possible modification according to the value of F_A for the current function A. It is found that the resulting pe regions generally depend on the order in which the functions are considered. To eliminate this arbitrariness, we impose yet another condition on the pe regions. We require that the order for treatment of these functions cause as large a proportion of phase space as possible to be assigned to pe regions. We find that this order is usually D, P, L, L^2, H_0, and the results reported here are obtained using this specific order.

As we have mentioned above, pe zones are not necessarily regions of predominant chaos. Since we are mainly interested here in pe regions containing chaotic motion, we seek a characteristic of the regions that indicates chaos. If we were dealing with true ergodicity instead of pe, we could examine the Liouville measure of the region; a value of zero would indicate a regular region (at least for systems with two degrees of freedom),[16–18] while a nonzero value would indicate a chaotic region. In a Poincaré surface of section plot, the measure would be reflected in the "width" of the region. A regular region, associated with an invariant torus, would show up as a one-dimensional curve of zero width while a chaotic region would appear as a more diffuse scatter of points of nonzero width. Unfortunately, this analysis does not apply to pe zones, since these generally have measures and Poincaré widths that are nonzero even when the motion is regular. To understand this point, consider a narrow regular region of phase space containing invariant tori with simi-

lar values for action variables. Motions on these tori yield similar values for the time averages $\overline{A(p(t),q(t))}^{\tau}$. Indeed, if the tori are sufficiently close to each other in phase space, it is easy to show that they will fall within the same pe region unless the set $\mathscr{A}$ includes the exact constants of motion for the system. Despite these comments, however, we expect the Poincaré widths or measures of such regular pe regions to be smaller than those bearing "large-scaled chaotic" motion, provided that $\mathscr{A}$ includes reasonably good approximate constants of motion. Thus, it should still be possible to classify most pe regions of interest here as regular or chaotic by examining their widths.

Poincaré widths of regular regions may be estimated from the rms deviations (taken over these regions) of the exact action variables. More generally, we expect the widths of both regular and chaotic regions to be roughly reflected in the rms deviations of approximate constants of motion. Empirically, we find that the rms deviation of property L,

$$\sigma_L = (\langle L^2 \rangle - \langle L \rangle^2)^{1/2} \tag{16}$$

is well suited for distinguishing regular from chaotic motion. Examination of Poincaré surfaces and calculation of maximal Lyapunov numbers for individual trajectories show that regions for which σ_L is greater than 1.6 are predominately chaotic while those for which σ_L is less than 1.6 are predominately regular. Thus, in order to restrict our present study to pe regions that are chaotic, we impose the condition $\sigma_L > 1.6$ upon these zones. Only regions that satisfy this test are considered here.

V. RESULTS

Figures 1–5 show Poincaré surfaces of section of the Henon–Heiles system at an energy of 25 (about 96% of the escape energy). Each of these plots is a composite obtained by selecting approximately 50 trajectories from a particular pe region and propagating them for 30 time units. Some of these figures resemble Poincaré surfaces for regular motion[13–25] associated with invariant tori. However, as emphasized above, the pe zones obtained here always contain predominately chaotic motion. Thus, the regions illustrated in these figures are vague tori[23]—approximately invariant regions that temporarily trap chaotic trajectories, rather than true tori—rigorously invariant regions that permanently hold regular trajectories. It is interesting to reflect on the parallel between vague tori, as regions of pseudoergodicity for chaotic motion and true tori, as regions of ergodicity for regular motion. To a certain extent, the pe concept allows us to quantify the notion of the vague torus.

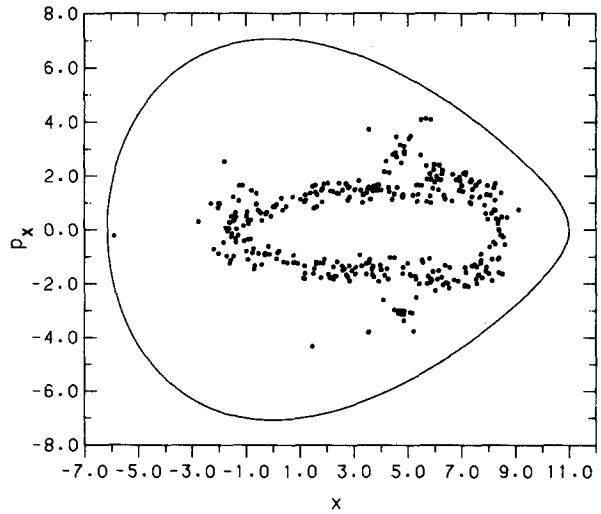

FIG. 2. A composite Poincaré surface of section of another precessing pseudoergodic region of the Henon–Heiles system with $E = 25.0$.

We now consider these figures in more detail. Figures 1 and 2 resemble Poincaré plots for regular precessing trajectories[25] of the Henon–Heiles system. Such trajectories have the characteristic of circulating around the potential energy surface and form one of the two main classes of regular trajectories for this system. Since the circulation may occur in the clockwise or counterclockwise sense, regular presessing trajectories occur in pairs. Our figures are reminiscent of the

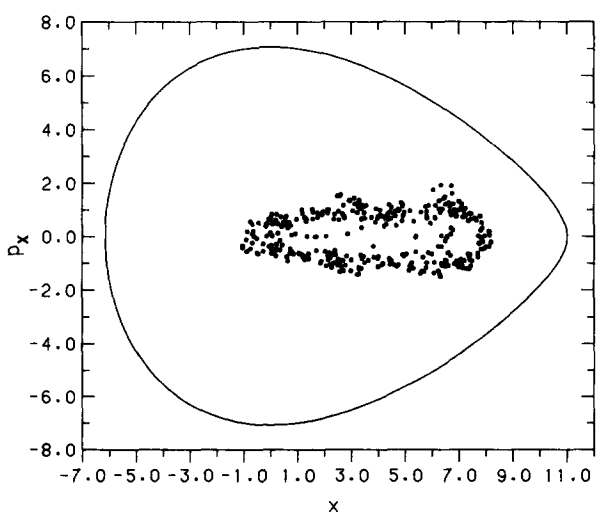

FIG. 1. A composite Poincaré surface of section of a precessing pseudoergodic region of the Henon–Heiles system with $E = 25.0$.

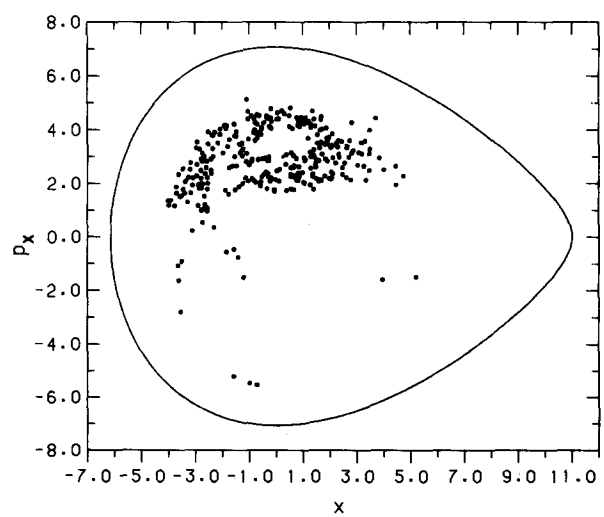

FIG. 3. A composite Poincaré surface of section of a librating pseudoergodic region of the Henon–Heiles system with $E = 25.0$.

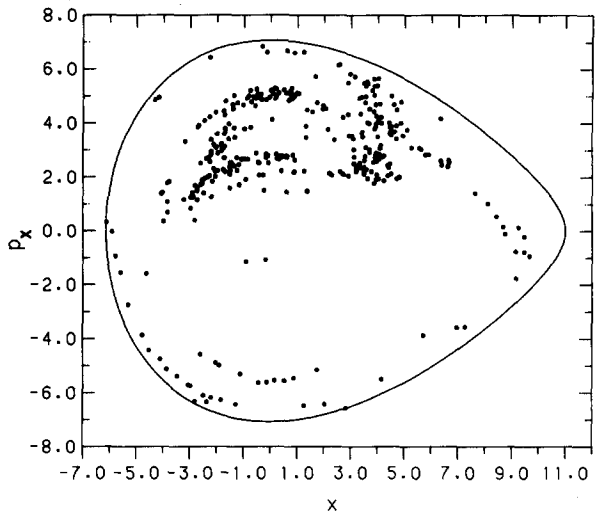

FIG. 4. A composite Poincaré surface of section of an unconventional librating pseudoergodic region of the Henon–Heiles system with $E = 25.0$.

Poincaré plots associated with regular motion in only one of the two senses. Regular motion in the opposite sense would form a crescent-shaped region in the empty area in the left portion of the figures. Indeed, the pe regions illustrated are members of pairs, the other member (not shown) forming crescent-shaped regions in the expected areas of the plots. The two pe regions that form a given pair have the same values for phase space averages $\langle A \rangle$ for all functions A considered except L. For this last function, the two regions have averages that are equal in magnitude but opposite in sign. Since L represents the angular momentum of the trajectories, the opposite signs of L are consistent with the opposite senses of motion for the constituent trajectories.

Figure 3 resembles the Poincaré plot for librating regular trajectories[25] of the Henon–Heiles system. These trajectories have the characteristic of being approximately confined to the C_2 axes of the potential and form the second main class of regular trajectories for this system. Since there are three C_2 axes (the potential has C_{3v} symmetry), librating trajectories occur in sets of three. Figure 3 is reminiscent of the Poincaré plot for only one of these three trajectories. One of the other two trajectories would form the mirror image of Fig. 3 in the bottom portion of the Poincaré plane and the last trajectory would form a sequence of points that lie around the periphery of the energetically allowed portion of the plane. In fact, the pe region illustrated is only one of three symmetry-related pe regions; the other two (not shown) are located in portions of the Poincaré plane similar to those described above for regular librators.

The three symmetry-related librating pe zones have the same values for $\langle L \rangle$, $\langle H_0 \rangle$, and $\langle L^2 \rangle$ but different values for $\langle D \rangle$ and $\langle P \rangle$. The symmetry relations among these regions are revealed by examining the polar-like quantities r and θ, defined by

$$r = (\langle D \rangle^2 + \langle P \rangle^2)^{1/2} \tag{17}$$

and

$$\theta = \tan^{-1}(\langle P \rangle / \langle D \rangle). \tag{18}$$

To obtain a geometrical interpretation of these quantities, we need to recognize that librating-like pe zones appear roughly elliptical in configuration space with a major axis that emanates from the center of the Henon–Heiles potential. It can be shown that r measures the "eccentricity" of this ellipse. A high value of r signifies that the trajectories are confined to a region that is rather close to the axis while a low value of r implies that the trajectories occupy a more diffuse region. The quantity θ, on the other hand, measures the orientation angle of the major axis of the ellipse from one of the C_2 axes of the potential. Not surprisingly, then, it is found that the three symmetry-related librating pe zones have the same value for r but values of 0, $2\pi/3$, and $4\pi/3$ for θ, indicating that the regions have the same shape but are oriented about different C_2 axes.

Figure 4 illustrates a pe region that looks much like the librating zone shown in Fig. 3. However, the pattern in Fig. 4 is more diffuse and there are now a substantial number of points that do not lie in the region expected of a regular librating trajectory. We call the region illustrated in Fig. 4 an unconventional librating zone. In contrast to conventional librating regions such as illustrated in Fig. 3, the unconventional zones appear to occur in symmetry-related sets of six.[26] Each member of such a set has the same values for $\langle L \rangle$, $\langle L^2 \rangle$, $\langle H_0 \rangle$, and r, but different values of θ. If we call the lowest absolute value of θ for these regions θ_0, then the values of θ for the six regions are $\pm\theta_0$, $2\pi/3 \pm \theta_0$, and $4\pi/3 \pm \theta_0$. It may thus be said that unconventional librators differ from conventional librators in that they have nonzero angles of orientation $\pm\theta_0$ about the C_2 axes. Another difference between the two kinds of zones can be established by close examination of Figs. 3 and 4: the unconventional regions lie closer to the (destroyed) main separatrix of the Henon–Heiles system.[13,25,27] This is a curve which separates the librating and precessing portions of the Poincaré plane. It is about this curve that large-scale chaos first appears as the energy of the system is raised.[27]

Figure 5 illustrates still another kind of pe region. Unlike the ones previously described, this region does not have

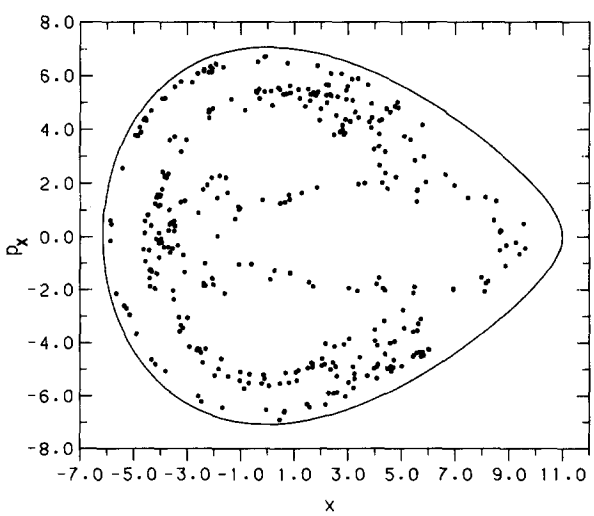

FIG. 5. A composite Poincaré surface of section of a global-like pseudoergodic region of the Henon–Heiles system with $E = 25.0$.

any symmetry-related partners. It appears to lie about the main separatrix and to be the most diffuse of the pe zones. We call such a region global-like.

We have located pe zones for the Henon–Heiles system at energies $E = 17.0, 17.5, 18.0, 18.5, \ldots, 26.5$. To summarize the results of these calculations, we present, in Figs. 6–9, plots of the phase averaged functions $\langle A \rangle$ vs energy for each of these zones. For now, attention should be focused on the open symbols which denote the classical results. The closed symbols, which represent quantum results, will be explained in Sec. IV. In these figures, circles, squares, diamonds, and triangles describe data for precessing, conventional librating, unconventional librating, and global-like pe zones, respectively. Examination of these results shows that different kinds of pe regions occupy different portions of these figures and thus have different characteristic values for the phase space averages. Precessing regions have relatively high values of $\langle L^2 \rangle$, low values of $\langle H_0 \rangle$, nonzero $\langle L \rangle$, and nearly zero values of r. In contrast, conventional librating pe zones tend to have relatively low values of $\langle L^2 \rangle$, high values of $\langle H_0 \rangle$, nearly zero value of $\langle L \rangle$, high values of r, and nearly zero values of θ_0. Unconventional librators have somewhat higher values for $\langle L^2 \rangle$ and lower values for $\langle H_0 \rangle$ than the conventional ones. Although both conventional and unconventional librators have nearly zero values of $\langle L \rangle$ and nonzero values of r, the values of r for the unconventional zones are lower than for the conventional regions and the values of θ_0 are nonzero. The phase averages for unconventional librators, thus, lie closer to the precessing values than do those for the conventional librators. The global-like zones are characterized by phase averages that lie still closer to the precessing regions. For these zones, the $\langle L^2 \rangle$ are lower and the $\langle H_0 \rangle$ are higher than for unconventional librators. As in the case of the librators, the $\langle L \rangle$ are nearly zero while, as in the case of

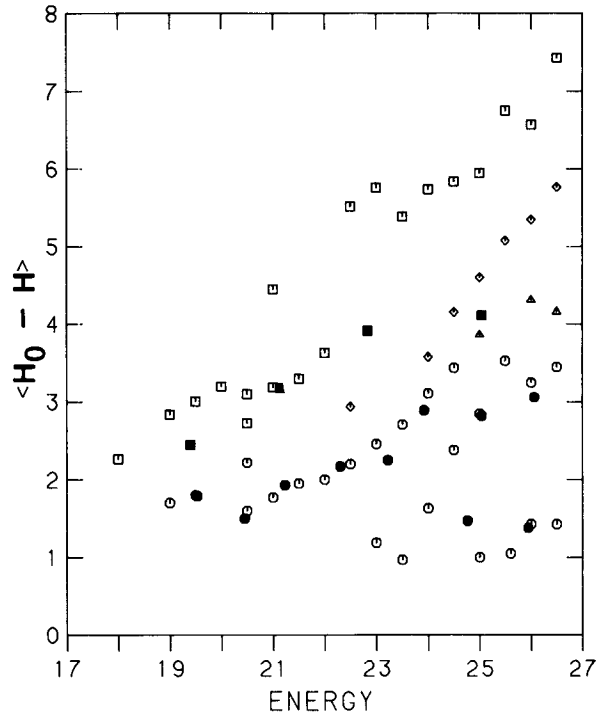

FIG. 7. Classical phase space averages $\langle H_0 - H \rangle$ and quantum phase space averages $\langle \hat{H}_0 - \hat{H} \rangle$ for pseudoergodic regions found at various energies of the Henon–Heiles system. The code for the symbols is as in Fig. 6. $\langle H_0 \rangle - E$ is plotted here instead of $\langle H_0 \rangle$ to avoid a secular increase in the values as a function of E.

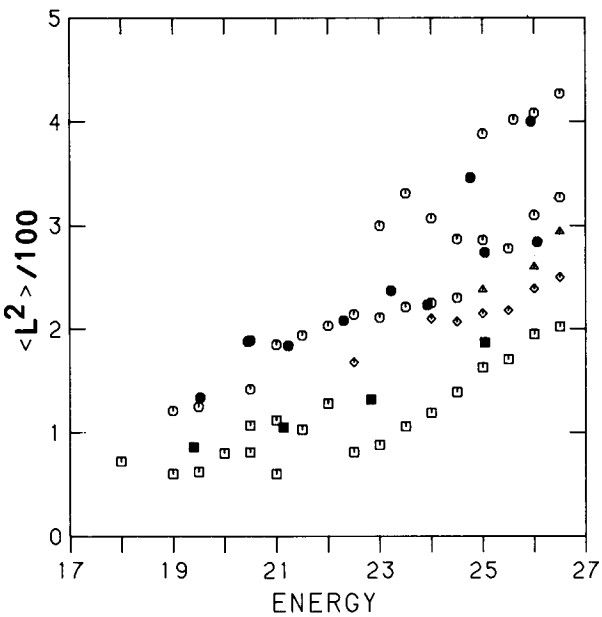

FIG. 6. Classical phase space averages $\langle L^2 \rangle$ and quantum phase space averages $\langle \hat{L}^2 \rangle$ for pseudoergodic regions found at various energies of the Henon–Heiles system. Unfilled symbols describe results for the classical regions: circles denote precessing regions, squares denote conventional librating regions, diamonds denote unconventional librating regions, and triangles denote global-like regions. Filled symbols describe results for the quantum regions: circles denote precessing-type regions and squares denote librating-type regions.

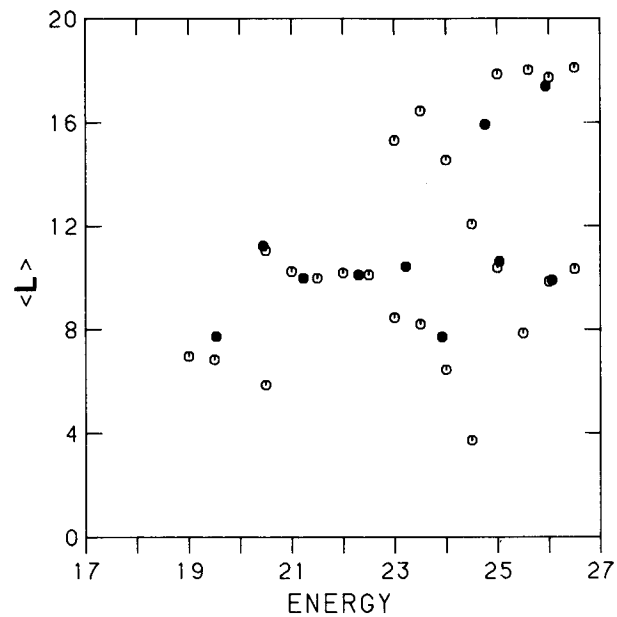

FIG. 8. Classical phase space averages $\langle L \rangle$ and quantum phase space averages $\langle \hat{L} \rangle$ for pseudoergodic regions found at various energies of the Henon–Heiles system. Only classical precessing zones (unfilled circles) and quantum precessing-type regions (filled circles) are indicated; the values for $\langle L \rangle$ and $\langle \hat{L} \rangle$ for the remaining regions are close to 0.

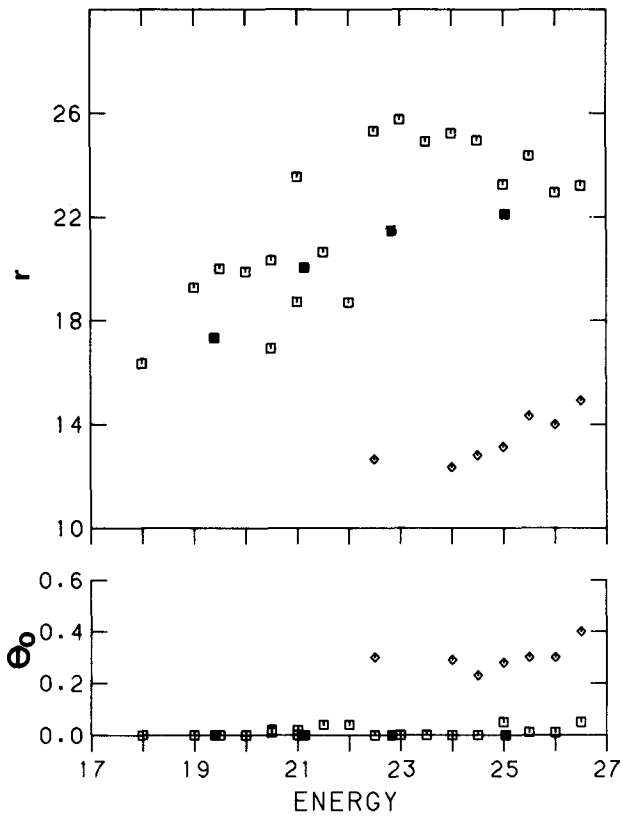

FIG. 9. Values of r and θ_0 for classical and quantum pseudoergodic regions at various energies of the Henon–Heiles system. Only classical conventional librating regions (unfilled squares), classical unconventional librating regions (unfilled diamonds), and quantum librating-type regions (filled squares) are indicated. For the remaining kinds of regions, r is close to 0 and θ_0 is not well defined.

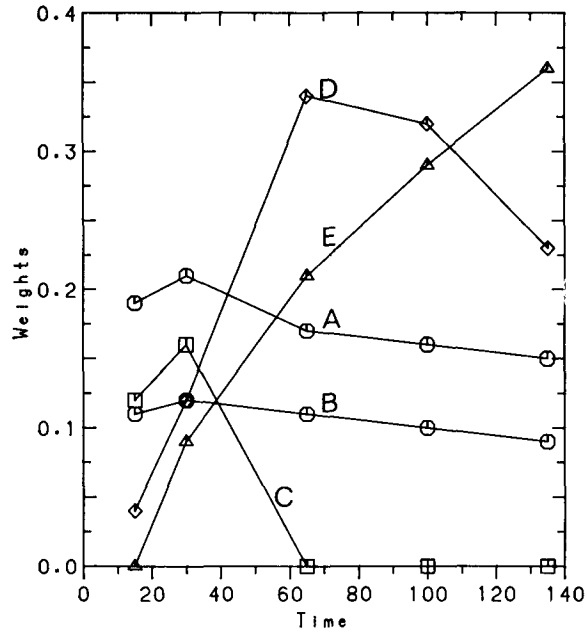

FIG. 10. The proportion of the energy surface occupied by various sets of symmetry-related pseudoergodic regions as a function of the observation time τ for the classical Henon–Heiles system with $E = 25.0$. (A) a set of high angular momentum precessing regions (see Fig. 2 for one such region at $\tau = 30$); (B) a set of low angular momentum precessing regions (see Fig. 1); (C) a set of conventional librating regions (see Fig. 3); (D) a set of unconventional librating regions (see Fig. 4); (E) the global-like region (see Fig. 5).

precessors, the r are nearly zero. These values, which are intermediate between those of librators and precessors, seem to characterize portions of phase space lying near the separatrix.

Closer inspection of the figures shows that there appear to be subfamilies within the precessing and librating areas that form separate patterns. The quality of the results makes it difficult to be certain but, at particular energies, some families seem to break off, bifurcate, or "collide" with others. It also seems that these phenomena are connected with the birth of new chains of unconventional librating and global-like families. Although we have not investigated these interesting subjects here in any detail, we believe that they merit future study.

We now investigate how these results depend on τ, the observation time. We find that different values of τ result in the same basic types of pe zones but that the relative sizes of these regions change. This is illustrated in Fig. 10 which describes results obtained at $E = 25.0$, the same energy used for Figs. 1–5. We recall that, at this energy, there are five different symmetry-related sets of pe zones for $\tau = 30$: two precessing sets, a conventional librating set, an unconventional librating set, and a global-like set. As τ is varied from 15 to 135, the sizes of the precessing regions remain roughly constant or slightly decrease, the size of the conventional librating set first increases and then decreases to 0 for $\tau > 30$, the size of the unconventional librating set rises from practically zero at $\tau = 15$ to a maximum near $\tau = 65$ and decreases for larger τ, while the size of the global-like zone increases monotonically with τ from a value of zero at $\tau = 15$ to the large value of 0.36 at $\tau = 135$. Thus, as τ increases, the measure of the global-like and unconventional librating regions increase at the expense of the conventional librators and, to a lesser extent, one of the precessors. This means that, as τ increases, the time averages of the functions in τ creep towards the separatrix values that characterize the latter two kinds of pe regions.

The variation in the sizes of the zones shows that the pe regions are generally *transitory phenomena*; the zones are not truly invariant, but only approximately invariant. Put another way, the boundaries that separate regions such as shown in Figs. 1–5 are not impervious barriers but, at best, bottlenecks that impede but do not totally stop phase space flow. Based on the analyses of other systems by other workers,[21,22] it seems probable that the regions illustrated in Figs. 1 and 2 are separated by a cantorus while it seems obvious that the regions shown in Figs. 2 and 3 are separated by the (destroyed) main separatrix of the system.

The observation that the global-like region becomes the largest single pe zone for large τ is worth discussing. Henon and Heiles[13] have shown that, when the energy of this system is equal to the escape energy, a single trajectory, propagated for a long time, "ergodically" visits most regions of the ener-

gy shell. The plot of the global-like pe region in Fig. 5 is, in fact, reminiscent of the Poincaré surface of that trajectory. Evidently, the emergence of the dominant global-like region for large τ is a manifestation of the phenomenon discussed by Henon and Heiles and signals the onset of ergodicity in a large portion of the energy surface.

Although these results are interesting, we must bear in mind that the pe regions described above are not unique. We recall that they were obtained by testing the condition $F_A < \phi$ with a particular ordering of the functions A. Although this ordering maximizes the proportion of pe regions on the energy surface, other possibilities certainly exist and these are found to generally result in different pe regions. Thus, when different orderings are used, the pe regions described above may reorganize, combine, or split up. In some cases, this results in pe zones of the kind already discussed but with altered values of the $\langle A \rangle$. In other cases, this causes the formation of new kinds of regions. For example, certain orderings result in the creation of "librating precessor" zones which appear to occur in symmetry-related sets of six and are characterized by nonzero values of $\langle L \rangle$ and r. Changes in the ordering tend to affect regions farthest from the main separatrix (precessors and conventional librators) to the least extent and those closest to this separatrix (unconventional librators, global-like regions, and librating precessors) to the greatest extent.

The observation that different procedures for locating the pe regions produce different results immediately raises the question of whether these regions (especially the ones near the separatrix) have any physical meaning. Since these regions are obtained by imposing the pe condition of Eq. (11), perhaps we should apply the question to the pe criterion itself. The pe condition, however, certainly does have physical significance. It describes an approximate, temporary form of ergodic classical behavior that can be imitated quantum mechanically. On the other hand, it is much more difficult to provide physical justification for our ordering of the functions A or for our choices of τ, ϕ, or $\mathscr{A}$; these are essentially arbitrary. Nevertheless, the imporant point for our purposes is that, once these choices have been made, the pe regions found are well-defined classical phenomena that should have quantum analogs for sufficiently small $\hbar$. Thus, having established the nature of the classical pe zones, we may inquire about the corresponding quantum behavior. We do this in the next section.

VI. COMPARISON WITH QUANTUM RESULTS

Although we have previously reported quantum calculations of pe zones for the Henon–Heiles system,[12] these are not exactly analogous to the present classical calculations since they resolve the nonuniqueness problem for the pe regions in a rather different way and do not take into account the current selection criterion of chaotic regions based on the value of σ_L. We therefore present a recalculation of the quantum pe zones.

We begin with a summary of the quantum pe concept. The quantum analog of the region $\mathscr{R}$ is formed by a set of at least two quantum states $|J\rangle$ having energy expectation values E_J that lie within the energy shell about E. This energy shell has a width σ that is determined by applying certain conditions described previously.[8,20] The density operator

$$\hat{\rho} = \sum_{J \in \mathscr{R}} |J\rangle \exp[-(E - E_J)^2/2\sigma^2] \langle J| \tag{19}$$

projects onto region $\mathscr{R}$. This operator must be chosen so that $\mathscr{R}$ obeys an approximate invariance condition that is analogous to the classical property described by Eq. (15). This condition, obtained by applying Wigner–Weyl[28] correspondence arguments, is found to be

$$|\langle \overline{\hat{A}(t)^\tau} \rangle - \langle \hat{A} \rangle| / [\langle |\hat{A}|^2 \rangle - |\langle \hat{A} \rangle|^2]^{1/2} < \beta \phi^{1/2} , \tag{20}$$

where $\hat{A}$ is the operator corresponding to classical function $A(p,q)$, $\hat{A}(t)$ is $\hat{A}$ propagated to time t in the Heisenberg picture, and

$$\langle \hat{A} \rangle = \mathrm{Tr}(\hat{\rho}\hat{A})/\mathrm{Tr}(\hat{\rho}) \tag{21}$$

is the quantum analog of the phase space average. Similarly, the analog of the classical function F_A, defined in Eq. (10), is found to be

$$F_A^q(T) = [\overline{\langle \hat{A}(t)^\dagger \hat{A} \rangle}^T - |\langle \hat{A} \rangle|^2] / [\langle |\hat{A}|^2 \rangle - |\langle \hat{A} \rangle|^2] . \tag{22}$$

The quantum condition that is analogous to the classical pe criterion is, thus,

$$F_A^q(\tau) < \phi \tag{23}$$

for all $A \in \mathscr{A}$ and with the same choices of τ, ϕ, and $\mathscr{A}$ as in the classical case.

As described previously,[12] insertion of complete sets of energy eigenstates into the traces of Eq. (22) results in an explicit formula for F_A^q in terms of the matrix elements of $\hat{A}$ and the energy eigenvalues [see Eq. (23) of Ref. 12]. This expression can be seen to be the quantum analog of Eq. (12) above and it is this formula that is actually used to calculate F_A^q. When this expression is substituted into Eq. (23), the pe condition is found to imply the following two conditions for matrix elements of $\hat{A}$: (a) expectation values $\langle J|\hat{A}|J\rangle$ are nearly independent of states $|J\rangle$ belonging to a pe region, and (b) off-diagonal matrix elements $\langle J|\hat{A}|K\rangle$ between states $|J\rangle$ in a pe region and states $|K\rangle$ with nearly equal energy are small. These are the analogs of the classical pe condition that the (finite) time averages of A are nearly independent of initial conditions in the pe zone.

By inserting complete sets of energy eigenstates into the traces appearing in Eq. (20), it becomes clear that the condition of approximate quantum invariance implies that the states $|J\rangle$ spanning $\mathscr{R}$ are either energy eigenstates or superpositions of such eigenstates with energy separations ΔE that are suitably small compared to $\hbar/\tau$. We find, in fact, that acceptable superpositions always have values of ΔE that *are less than $\hbar/\tau$. Thus, a practical way to find invariant regions is to form various superpositions $|J\rangle$ obeying $\Delta E < \hbar/\tau$*, use these superpositions to define density operators $\hat{\rho}$, and test for satisfaction of the invariance condition by substituting these operators into Eq. (20).

The computational procedure for partitioning the energy shell into quantum pe zones, in close analogy to the classical method, is as follows. We take the states in the quantum

energy shell, form various superpositions $|J\rangle$, and consider various groupings of two or more of such $|J\rangle$ into tentative pe regions. We identify the largest such region that obeys the approximate invariance and pe conditions. We then remove the states belonging to this region from the energy shell and repeat the above procedure with the remaining states. We continue identifying and removing the largest regions until all pe regions have been removed. The collection of pe regions identified (and subsequently removed) in this way is to be compared with the classical set of pe regions. If, at a given stage of this procedure, an ambiguity arises because there are two or more equally large regions that are candidates for consideration, the one ultimately causing the largest number of states to be assigned to pe regions is taken as the correct choice. Finally, we examine the quantity

$$\sigma_L^q = [\langle \hat{L}^2 \rangle - \langle \hat{L} \rangle^2]^{1/2} \tag{24}$$

for each of the pe regions in our set and reject regions with $\sigma_L < 1.6$ as involving predominately regular motion. The remaining pe regions should then be closely analogous to the chaotic pe zones obtained by our classical technique.

We have carried out the above procedure for the quantum Henon–Heiles system described by Eq. (13) with $\hbar = 1$. This system has 374 states with energies below the escape energy. Details concerning the diagonalization of this Hamiltonian have been presented previously.[12] The set $\mathscr{A}$ of functions used for the quantum calculations is the same as the classical set [Eqs. (14)] except that P is omitted. Since the sole effect of including this function in the classical calculations is to distinguish between different symmetry-related librators and since this can be done by inspection in the quantum calculations, the omission is not expected to influence the quantum-classical comparisons. The energy shell width σ is chosen as in Ref. 12.

As discussed in Ref. 12 and further elaborated below, symmetry considerations and the invariance requirement greatly restrict the choice of superposition states that can participate in pe regions. Thus, there are only three possible candidates for the states $|J\rangle$: (a) complex energy eigenstates of E symmetry or certain complex linear combinations of nearly degenerate pairs of eigenstates of A_1 and A_2 symmetry; (b) certain real linear combinations of two degenerate states of E symmetry with a single nearly degenerate state of A_1 or A_2 symmetry; (c) uncombined energy eigenstates. The coefficients for the different kinds of superpositions are presented in Ref. 12. States of the first and second kinds are called, respectively, precessing-type and librating-type states since they are expected, on the basis of symmetry, to form pe regions that correspond to their names. Precessing-type states occur in symmetry-related sets of two while librating-type states occur in symmetry-related sets of three. States of the third kind might be considered as candidates for the formation of global-like pe regions.

The quantum pe zones in our previous calculations[12] were identified by applying the alternative invariance condition $\Delta E < \hbar/\tau$ instead of the current condition expressed by Eq. (20). As we have mentioned above, this alternative condition appears to be less strict than the one applied here. Nevertheless, to allow comparisons to our earlier work and to establish some other points, we first present results for quantum pe regions obtained using the weaker invariance condition of $\Delta E < \hbar/\tau$ and then describe how these results change when Eq. (20) is imposed.

Figure 11 shows the states involved in pe zones. Symbols at coordinates $(n,|l|)$ represent energy eigenstates that have been assigned zero-order quantum numbers $n = 0, 1, 2,...$ (the principle quantum number) and $l = -n, -n+2,...,n$ (the angular momentum quantum number). The detailed assignments are described in Ref. 12. In this figure, a small diamond represents a state that does not participate in pe zones. A circle denotes a pair of symmetry-related precessing-type states. Such states can be denoted by a single symbol centered about a particular value of n and l since, even when these are superpositions of A_1 and A_2 states, both such states have the same n and l quantum numbers. A chain of these circles, connected by a solid line, denotes two pe regions formed from the two symmetry-related kinds of precessing-type states. A pair of boxes connected by a dotted line denotes three symmetry-related librating-type superpositions and a chain of such pairs connected by a solid line represents three pe regions formed from such states. Note that there are no pe zones that are formed from uncombined energy eigenstates. The inability to form such regions has been discussed in Ref. 12.

Pseudoergodic zones are concentrated in two main areas of Fig. 11. Regions formed from librating-like states are clustered towards the left of the figure, while regions formed from precessing-like states are located towards the right of the figure. This arrangement is consistent with the expectation, based on classical mechanics, that librating motion should occur in phase space regions of low angular momentum (low l) and precessing motion should occur in regions of higher angular momentum (high l). (Also see the classical values of $\langle L^2 \rangle$ for precessing and librating pe zones in Fig. 6.) Areas devoid of pe regions are found along the top, the left-most edge, the right-most edge, and in an approximately vertical strip passing through the middle of the figure. The absence of chaotic pe regions along the top is consistent with classical expectations since low n corresponds to energies below the threshold for the onset of large-

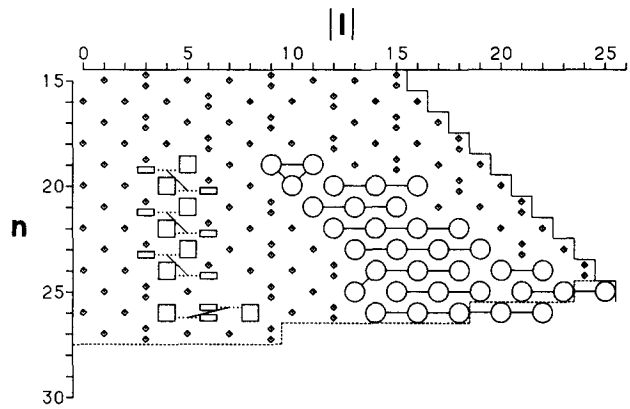

FIG. 11. States spanning the chaotic pe regions of the Henon–Heiles system. The broken curve at the bottom of the figure separates states above and below the escape energy. The remaining symbols are explained in the text.

scale chaos.[13] Similarly, the blank area to the right of the figure has a classical analog as discussed in Ref. 12. The absence of pe zones along the left edge and through the midportion of the figure are, however, nonclassical effects and will be discussed in greater detail below.

Figure 11 differs in some respects from Fig. 4 of Ref. 12 which presents similar information. There are fewer pe regions in the current figure and these regions do not always consist of the same states as described previously. One reason for the differences is that the condition $\sigma_L^q > 1.6$ was not invoked in the earlier work since it was assumed that the requirement for quantum pe regions to consist of at least two states would lead to zones that are "wide" enough to be chaotic. In the present work, however, we have found that this assumption is not always borne out. Imposing the minimum width condition on the pe zones serves to eliminate several regions found previously. A second reason for the differences between Fig. 11 and Fig. 4 of Ref. 12 is that the present criterion for formation of pe zones differs from that used previously. Instead of attempting to partition the energy shell so that as many states as possible are included in pe regions, as in Ref. 12, we adopt a procedure that is more directly analogous to the classical technique for identifying pe regions: we attempt to form pe regions that are individually as large as possible and only secondarily try to assign as many states as possible to pe regions when this recipe leads to ambiguities. Changing this procedure changes some of the resulting pe zones. This sensitivity of the results shows that the quantum pe regions are nonunique in the same sense as the classical regions.

The quantum ensemble-averaged values for the operators $\hat{A}$ are plotted in Figs. 6–9 along with the classical phase space averages. Filled circles denote values obtained for precessing-type states, while filled squares represent values obtained for librating-type states. Although quantum averages of P have not been explicitly calculated, their values can be deduced from symmetry considerations and the plot for θ_0 in Fig. 9 is obtained from these values.

As we have already mentioned, all the preceding quantum results were obtained using $\Delta E < \hbar/\tau$ as the invariance condition instead of Eq. (20). We now discuss how these results change when, in closer analogy with the classical calculations, Eq. (20) is used as the invariance condition and β is set equal to 1. We find that applying the latter condition has no effect on the quantum regions formed from precessing-type states; the identity of these zones and their values for $\langle \hat{A} \rangle$ remain unchanged from the results reported in Figs. 6–9. However, application of this invariance condition does have a significant effect on the quantum regions formed from librating-type states; none of these regions satisfy this stricter invariance condition so that none of these regions survive as legitimate pe zones. Strictly speaking, then, all results presented above for such regions should be disregarded. It is worth noting, however, that these regions do not fail this invariance test by very large margins. In fact, these regions do satisfy the invariance requirement of Eq. (20) if β is increased to the range of 2–5. Since we have found that the classical librating zones do not change drastically when they are required to obey the invariance condition with such values of β, comparisons of the quantum librating zones to the classical regions are still of interest. Thus, although we discuss below the reasons these quantum zones fail the invariance condition, we continue to treat these zones as valid pe regions for most purposes.

We now proceed with a comparison of the classical and quantum results for the ensemble averages $\langle A \rangle$, as presented in Figs. 6–9. Comparison of the filled and open circles in these figures shows that there is good quantum-classical agreement in the case of precessing motion. The quantum pe regions formed from precessing-type states are characterized by average values for the functions A that are similar to those for the classical precessing regions. This shows that the quantum precessing-type regions are indeed analogous to classical precessing regions. Comparison of the filled boxes with the open boxes, however, indicates that there is less satisfactory quantum-classical agreement in the case of librating motion. The quantum pe regions formed from librating-type states tend to have average values that are not very close to those of classical librating pe zones. Instead, they tend to be displaced toward the separatrix area of the figures (i.e., in the direction of areas occupied by classical precessing states). In particular, a family of classical librating regions with high energy, low $\langle L^2 \rangle$, high r, and high $\langle H_0 \rangle$ is represented very poorly, if at all, by the quantum results. As discussed below, these quantum-classical discrepancies are also responsible for the nonergodic region that appears on the far left of Fig. 11. Finally, neither the filled circles nor the filled boxes of Figs. 6–9 consistently lie in areas occupied by open diamonds and triangles. Thus, we have not identified quantum analogs of the unconventional librators or the global-like regions. The absence of analogs to these regions shows up in Fig. 11 as the nonergodic vertical strip through center of the diagram. Because the analogs to such regions are missing, the quantum pe regions occupy a smaller proportion of the energy shell than do the classical zones.

The question that naturally arises here is whether we have indeed examined all possible kinds of superposition states that can form quantum pe zones. Might certain, unexplored, linear combinations $|J\rangle$ of energy eigenstates be used to construct quantum pe zones that are analogous to the classical unconventional librating or global-like regions? The answer, for the value of Planck's constant investigated here, appears to be no. The pe condition $F_A^q < \phi$ together with the invariance condition and restrictions due to symmetry practically rule out linear combinations other than those already mentioned. For example, to construct quantum analogs of the unconventional librating regions, it would be necessary to form superpositions of at least six states since these classical regions occur in sets of six. However, inspection of eigenvalues reveals the energy range $\hbar/\tau$ never contains six consecutive energy levels of the required symmetry, so that superpositions cannot be formed that obey even the lenient invariance requirement. Similarly, attempts to form the analogs of global-like regions from superpositions of energy eigenstates (instead of individual, uncombined, eigenstates) fail because, to eliminate large off-diagonal matrix elements between states in the pe region and other states, as required by the pe condition, eigenstates that lie farther apart in ener-

gy than $\hbar/\tau$ would have to be included in the superpositions. Thus, any quantum regions resembling classical unconventional librating and global-like zones would violate the invariance condition much more seriously than do the quantum conventional librating zones. The conclusion that emerges is that there really are no quantum analogs to the unconventional librating or global-like classical pe zones for the present value of $\hbar$.

We now discuss the discrepancies between the quantum and classical results. First, we address the inability of the quantum librating zones to obey the same invariance condition as the classical regions. The lack of invariance of the quantum regions, as reflected in the failure of Eq. (20), can be traced to the relatively large values of energy splittings ΔE between the pairs of levels of E and A_1 or A_2 symmetry which combine to form states $|J\rangle$ spanning these regions. In the case of regular motion, these splittings are associated with quantum tunneling between the three symmetry-related librating regions and it is reasonable to assume that the same association often remains valid in the case of chaotic motion. This tunneling phenomenon, which occurs on the relatively short time scale of $\hbar/\Delta E$, leads to a breakdown of the quantum-classical agreement for the dynamics of the functions $A \in \mathscr{A}$ during the observation time $\tau = 30$. For this reason, agreement between classical and quantum pe for librating cases is, at best, restricted to smaller values of τ or to regions obtained with larger values of β.

This discussion does not, however, explain why none of the quantum librating regions we have found form adequate analogs of the classical librating pe regions with low $\langle L^2 \rangle$, high r, and high $\langle H_0 \rangle$. We, therefore, turn our attention to this matter. If quantum regions analogous to these classical zones were present, they would lie in the leftmost portion of Fig. 11 where quantum pe regions are currently absent. In fact, Fig. 4 of Ref. 12 shows that quantum pe zones *are* present in this area of (n,l) space. These regions are not displayed in Fig. 11 because they have values of σ_L^2 that are less than 1.6 and are thus considered to be nonchaotic. Nonchaotic quantum pe regions with $n < 21$ appear to have classical analogs since our calculations show that there exist classical nonchaotic pe zones having $E \simeq n + 1 < 22$ and values of the $\langle A \rangle$ that are somewhat similar to those of the $\langle \hat{A} \rangle$. However the agreement between these quantum and classical averages is not really very close for these zones (e.g., the values for the $\langle \hat{L}^2 \rangle$ are too low) so that the analogs are not very accurate ones. On the other hand, nonchaotic quantum pe zones with low l and $n > 21$ do not have classical analogs at all since every librating classical pe region in this energy range that is large enough to show up quantum mechanically is chaotic. These chaotic classical regions, in fact, form part of the librating series with low $\langle L^2 \rangle$, high r and high $\langle H_0 \rangle$ that is not reproduced quantum mechanically. The conclusion we reach is that the states on the far left of Fig. 11, and especially those with high energy, behave very nonclassically. They do not display symptoms associated with classical chaos such as the tendency to form pe regions that spread out and attain relatively large Poincaré widths.

This nonclassical behavior is very reminiscent of a phenomenon that occurs in other quantum mechanical systems of coupled oscillators[19(a),29] and that we have called quantum trapping. When such systems are prepared at energies close to the escape energy, with high energy in an anharmonic degree of freedom and low energy elsewhere, they are found to remain trapped in that initial state long after the classical counterpart evolves to other regions. The "reduced degree of ergodicity"[19(a)] that describes such quantum behavior has been explained[19(a)] to be a result of the narrowness of the nonlinear resonances that are responsible for the classical chaos in this region of phase space. An alternative explanation,[30] that may be complementary to the one above, is that the classical flux out of the trapping region is lower than h[22,31-33] so that the classical escape from these zones is quantum mechanically irrelevant.[34] Since the Henon–Heiles states under consideration are indeed characterized by a total energy near the escape energy with most of this energy concentrated in an anharmonic degree of freedom, we believe that the nonclassical behavior observed here is an example of the trapping effect.

The above discussion helps explain the observation that the $\langle \hat{A} \rangle$ values of the quantum librating zones lie closer to the separatrix regions of Figs. 6–9 than do those of the classical zones. The quantum states discussed in the previous paragraph have values for the $\langle \hat{A} \rangle$ that lie farthest from the separatrix region of Figs. 6–9. Presumably, were it not for the trapping effect, these states would contribute to quantum pe zones resembling those classical pe librating regions that are farthest from the separatrix. However, the trapping effect prevents these states from participating in the formation of such regions. Removal of these states from the quantum librating zones causes the "center of gravity" of these regions to shift toward the separatrix.

In a similar way, the trapping effect may provide an alternative explanation for the lack of invariance of the quantum librating regions. In contrast to these chaotic regions, we find that the nonchaotic quantum librating pe regions, associated with trapping, satisfy the invariance condition of Eq. (20) very well. The effective removal of the trapping states from the quantum librating regions may decrease the mean invariance time of the resulting zones, causing them to fail the invariance test.

We now discuss the absence of quantum analogs to the unconventional librating and global-like regions. Although this may be, in part, an indirect consequence of the trapping effect for the librating states, we believe that it is a separate phenomenon. The probable cause for the quantum-classical discrepancies for these regions is that their formation times are longer than the maximum time scale of close correspondence between classical and quantum mechanics. Indeed, Fig. 10 suggests the global-like and unconventional librating zones take somewhat longer to become large than do the precessing and conventional librating regions. However, there is reason to suspect that the problem is not so much that the formation time for these zones is too long as that the quantum-classical correspondence time for these regions is exceptionally short. Indeed, as we have discussed briefly above, the main obstacle to the formation of such quantum pe regions is that the energy separations between states which must be superposed to span such regions are too great

for the invariance criterion to be obeyed. Since the classical regions certainly appear to be large enough by time 30 for their quantum analogs to exist, a quantum mechanical effect seems to be at work causing level separations to be unusually large, thus limiting the correspondence time. This effect may, again, be a tunneling phenomenon. Strong tunneling is, in fact, expected for unconventional librating and global-like regions since these lie near the separatrix which marks a kind of barrier maximum in phase space. Apart from the tunneling between different symmetry-related librating regions discussed above, states in the present regions may also undergo appreciable tunneling between librating and precessing regions and, perhaps, more complicated forms of tunneling, as well. Additional evidence that the states near the separatrix are severely affected by tunneling comes from the difficulty in assigning zero-order (n,l) quantum numbers to these states,[12] the irregular progression of expectation values for these states as a function of l,[35] and the presence of energy level curve crossings, as a function of λ,[35] between these states and others with very different quantum numbers.[36] It is possible that purely classical treatments of unconventional librating and global-like regions are necessarily inaccurate and that approaches on at least the semiclassical level are needed to describe the quantum behavior in this portion of phase space.

Figure 12 is the quantum analog of Fig. 10 and shows how the sizes of the quantum pe zones near $E = 25.0$ vary with τ. At this energy, the quantum mechanical system has, at most, two precessing pe regions and one librating pe region. Comparison with Fig. 10 shows that the agreement between the sizes of the quantum and classical regions is not very good. One reason for this is that the quantum relative weights plotted in Fig. 12 were obtained by the crude procedure of dividing the number of states in the regions by the total number of states falling within the width of the energy shell. Reference 12 describes a method that would be expected to yield more accurate agreement with classical weights. A second reason for the unimpressive quantum-classical agreement for regions sizes is that these regions consist of only a few quantum states so that even uncertainties on the order of one state cause large relative changes in their sizes. Despite these differences, however, Figs. 10 and 12 show some important similarities. In both cases the sizes of the precessing regions remain approximately independent of τ over the full range of values explored. Also, in both cases, the size of the librating regions first increases and then decreases to 0 as τ is increased. However, unlike the classical case, the quantum mechanical system displays no compensating growth in the sizes of unconventional librating and global-like regions as the librating zones get smaller. The observation that such quantum regions do not appear even at large τ, when their classical counterparts occupy one-third of the energy surface, again confirms that their absence is not due to their small size relative to h^2 but to the short classical-quantum correspondence time relative to the time scale required for the formation of these zones.

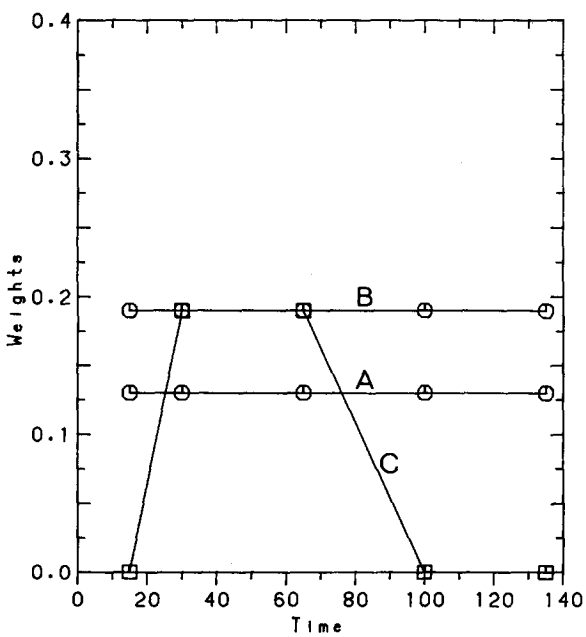

FIG. 12. The proportion of the energy shell occupied by various sets of symmetry-related pseudoergodic regions as a function of the observation time τ for the quantum Henon–Heiles system with $E = 25.0$. (A) high angular momentum precessing-type regions; (B) low angular momentum precessing-type regions; (C) librating-type regions.

Classically, the precessing and librating pe zones account for only a minor part of the chaotic region of phase space. For large τ, much of the remaining part of the chaotic region is occupied by unconventional librating zones and, especially, the single global-like zone. We should again recall the Poincaré map of Henon and Heiles[13] at the escape energy and its apparent relation to this global-like zone. The implication of our results is that the truly large scale classical ergodic behavior represented by the Henon–Heiles Poincaré plot does not occur in our quantum system.

VII. SUMMARY AND CONCLUDING REMARKS

We have described the concept of psuedoergodicity in classical systems and have introduced a computational technique to identify classical pe regions. In rough physical terms, a pe region is a nearly invariant portion of phase space consisting of points that are close to a single trajectory of finite duration. We have investigated the chaotic pe regions of the highly excited Henon–Heiles system and have found that these zones sometimes resemble precessing and librating invariant regular portions of phase space. Such regions can be identified with the vague tori of Reinhardt and coworkers.[23] It is reasonable to infer that such zones are separated from each other by bottlenecks that impede phase space flow. Other pe regions, located closer to the main separatrix of the system, have less familiar forms and are referred to by names such as unconventional librating zones and global-like zones. As the observation time for definition of the pe zones is increased, a single global-like region becomes progressively larger and begins to dominate phase space. This marks the transition from pseudoergodicity to ergodic behavior in a region that encompasses much of the energy surface of the system.

Our main motivation for introducing the pe concept has been to describe a form of ergodic-like behavior that should

be more clearly reflected in quantum mechanics than is ergodicity itself. Accordingly, we have compared the classical pe zones of the Henon–Heiles system to those obtained from a corresponding quantum mechanical definition. In the course of this comparison, we have verified most of the conclusions of our earlier quantum treatment of pe.[12] In particular, we have confirmed that the presence of quantum pe regions often does reflect the existence of analogous classical pe zones and have verified that there are, indeed, certain classical pe regions that do not show up quantum mechanically. Our present calculations have, however, taken us beyond the inferences of our earlier study by identifying precisely which classical zones fail to appear in the quantum mechanical system. These classical regions include the chaotic librators that are farthest from the main system separatrix and the unconventional regions that form near this separatrix. The absence of these pe regions in the quantum system appears to be due, in one way or another, to the short time for quantum-classical correspondence for the current value of $\hbar$. The lack of quantum pe regions that are analogous to the classical global-like zones rules out behavior resembling large-scale classical ergodicity for the quantum system. A similar result for real molecules might prevent application of the usual statistical theories of kinetics even though they were valid classically.

The computational technique we have used to examine the trajectories and identify the classical pe regions is of independent interest and may have applications in other areas. For example, to the extent that this method identifies regions separated by dynamical bottlenecks, it may prove useful for carrying out classical transition state calculations of intramolecular vibrational energy transfer.[22] The method may be particularly useful for systems having more than two degrees of freedom since current techniques have difficulties in such cases. An application that we have already begun to investigate[35] uses the present technique to sort chaotic trajectories that are obtained by adiabatic switching of zero-order invariant tori. We have found that the largest resulting pe zones often bear a closer relationship to the quantum states of the system than do the unsorted trajectories.

ACKNOWLEDGMENT

We gratefully acknowledge the support of this research by the National Science Foundation through Grant CHE-8418170.

APPENDIX: THE TRAJECTORY SORTING PROCEDURE

Here we present details of the computational procedure for identifying classical pe zones given the time averages $\overline{A(p(t),q(t))^\tau}$ for a set of trajectories.

(1) Choose a particular order in which to examine the functions A. For example, in the present work, this order was chosen to be $D, P, L, L,^2 H_0$. These functions are, henceforth, referred to as functions 1,2,...,N.

(2) To each function, associate a list of trajectories that qualify for the pe region presently being formed. The list for function 1 initially contains all trajectories. The list for the remaining functions is initially blank.

(3) Carry out the following steps for function 1:

(a) Create a histogram of $\overline{A(p(t),q(t))^\tau}$ values for the trajectories in the list of the function. Form a pe region consisting of a pair of trajectories selected from the maximum of the histogram. Calculate F_A. Keep enlarging the group by adding trajectories ever farther from the maximum of the histogram until the condition $F_A < \phi$ is no longer satisfied.

(b) If the group obtained above is large enough to correspond at least two quantum states:

(i) If the function being considered is not function N, the members of this group form a list of trajectories for the next function. Return to step (a) for the next function.

(ii) If the function being considered is function N:

(1) Delete those trajectories from the list of the function that have large values of $|\langle \overline{A(t)^\tau} \rangle - \langle A \rangle|$ until the invariance condition, Eq. (15), is obeyed.

(2) If the resulting group is too small to correspond to at least two quantum states, go to step (c) (ii).

(3) If the resulting group is large enough to correspond to at least two quantum states, this group forms a pe region. Delete the members of this group from the list of function 1. Then, return to step (a) for function 1 to identify additional possible pe regions.

(c) If the group is too small to correspond to at least two quantum states:

(i) If the function being considered is function 1, quit.

(ii) If the function being considered is not function 1, remove from the list of the previous function a small proportion of trajectories that originally arose from the region near the histogram maximum of that function (the proportion used in our calculations was typically 1/8 but the results were not very sensitive to this value). Then return to step (a) for the previous function.

[1] V. I. Arnold and A. Avez, *Ergodic Problems in Classical Mechanics* (Benjamin, New York, 1969).
[2] I. E. Farquhar, *Ergodic Theory in Statistical Mechanics* (Interscience, London, 1964).
[3] P. Walters, *An Introduction to Ergodic Theory* (Springer, New York, 1982).
[4] A. J. Lichtenberg and M. J. Lieberman, *Regular and Stochastic Motion* (Springer, New York, 1983).
[5] See, e.g., W. Forst, *Theory of Unimolecular Reactions* (Academic, New York, 1973).
[6] A. I. Schnirelman, Usp. Mat. Nauk **29**, 181 (1974).
[7] A. Voros, in *Stochastic Behavior in Classical and Quantum Systems*, edited by G. Casati and J. Ford (Springer, Berlin, 1979).
[8] K. G. Kay, J. Chem. Phys. **79**, 3026 (1973).
[9] E. B. Stechel and E. J. Heller, Annu. Rev. Phys. Chem. **35**, 563 (1984).
[10] E. B. Stechel, J. Chem. Phys. **82**, 364 (1985).
[11] P. Pechukas, J. Phys. Chem. **88**, 4823 (1984).
[12] B. Ramachandran and K. G. Kay, J. Chem. Phys. **86**, 4628 (1987).
[13] M. Henon and C. Heiles, Astron. J. **69**, 73 (1964).

[14]A. preliminary description of some of these results has been presented in: K. G. Kay in *Proceedings of The Fritz Haber International Symposium on: "Chaos and Related Nonlinear Phenomena--Where do we go from here?"*, edited by I. Procaccia and M. Shapiro (Plenum, New York, to be published).
[15]See Ref. 4, p. 285.
[16]G. Contopolous, L. Galgani, and A. Giorgilli, Phys. Rev. A **18**, 1183 (1978).
[17]S. C. Farantos and J. Tennyson, J. Chem. Phys. **84**, 6201 (1986).
[18]H. V. Kuz'min, I. V. Nemov, A. A. Stuchebrukhov, V. N. Bagratashvili, and V. S. Letokhov, Chem. Phys. Lett. **124**, 502 (1986).
[19]See, e.g., (a) K. G. Kay, J. Chem. Phys. **72**, 5955 (1980); (b) M. J. Davis and E. J.Heller, *ibid.* **80**, 5036 (1984).
[20]B. Ramachandran and K. G. Kay, J. Chem. Phys. **83**, 6316 (1985).
[21]R. S. MacKay, J. D. Meiss, and I. C. Percival, Physica D **13**, 55 (1984); D. Bensimon and L. P. Kadanoff, *ibid.* **13**, 82 (1984).
[22]M. J. Davis, J. Chem. Phys. **83**, 1016 (1985); M. J. Davis and S. K. Gray, *ibid.* **84**, 5389 (1986); S. K. Gray, S. A. Rice, and M. J. Davis, J. Phys. Chem. **90**, 3470 (1986).
[23]R. B. Shirts and W. P. Reinhardt, J. Chem. Phys. **77**, 5204 (1982); C. Jaffé and W. P. Reinhardt, *ibid.* **77**, 5191 (1982).
[24]See the discussion concerning Figs. 1 and 2 of Ref. 12.
[25]D. W. Noid and R. A. Marcus, J. Chem. Phys. **67**, 559 (1977).
[26]The trajectory sorting technique does not always identify all six of these regions. The number and identity of the regions that are actually found depends on the order in which the functions A are treated.
[27]G. Walker and J. Ford, Phys. Rev. **188**, 416 (1969).
[28]E. Wigner, Phys. Rev. **40**, 749 (1932); R. Balescu, *Equilibrium and Nonequilibrium Statistical Mechanics* (Wiley, New York, 1975).
[29]S. N. Rai and K. G. Kay, J. Chem. Phys. **80**, 4961 (1984).
[30]M. J. Davis (private communication).
[31]R. C. Brown and R. E. Wyatt, Phys. Rev. Lett. **57**, 1 (1986), J. Phys. Chem. **90**, 3590 (1986).
[32]T. Geisel, G. Radons, and J. Rubner, Phys. Rev. Lett. **57**, 2893 (1986).
[33]L. L. Gibson, G. C. Schatz, M. A. Ratner, and M. J. Davis, J. Chem. Phys. **86**, 3263 (1987).
[34]The trapping phenomenon may also be related to the success of the adiabatic approximation for these states. See K. Stefanski and H. S. Taylor, Phys. Rev. A **31**, 2810 (1985); Y. Y. Bai, G. Hose, K. Stefanski, and H. S. Taylor, *ibid.* **31**, 2821 (1985).
[35]B. Ramachandran and K. G. Kay (unpublished).
[36]See, e.g., E. J. Heller, Faraday Discuss. Chem. Soc. **75**, 141 (1983) for a discussion of the significance of such crossings.